

promoting access to White Rose research papers



Universities of Leeds, Sheffield and York
<http://eprints.whiterose.ac.uk/>

This is an author produced version of a paper published in **Physics of Plasmas**.

White Rose Research Online URL for this paper:

<http://eprints.whiterose.ac.uk/8736/>

Also available from arXiv <http://arxiv.org/abs/0812.0697>

Published paper

Kim, E.J., Liu, H.L. and Anderson, J. (2009) *Probability distribution function for self-organization of shear flows*. *Physics of Plasmas*, 16 (5). Art. No.052304.

<http://dx.doi.org/10.1063/1.3132631>

Probability distribution function for self-organization of shear flows

Eun-jin Kim, Han-Li Liu¹, and Johan Anderson

Department of Applied Mathematics,

University of Sheffield, Sheffield, S3 7RH, U.K.

¹*High Altitude Observatory, National Center for
Atmospheric Research, Boulder CO 80307, USA*

Abstract

The first prediction of the probability distribution function (PDF) of self-organized shear flows is presented in a nonlinear diffusion model where shear flows are generated by a stochastic forcing while diffusing by a nonlinear eddy diffusivity. A novel non-perturbative method based on a coherent structure is utilized for the prediction of the strongly intermittent exponential PDF tails of the gradient of shear flows. Numerical simulations using Gaussian forcing not only confirm these predictions, but also reveal the significant contribution from the PDF tails with a large population of super-critical gradients. The validity of the nonlinear diffusion model is then examined using a threshold model where eddy diffusivity is given by discontinuous values, elucidating an important role of relative time scales of relaxation and disturbance in the determination of the PDFs.

I. INTRODUCTION

Many important phenomena in nature are often far from equilibrium, strongly driven by instabilities or by external forces. Examples are diverse, from forest-fires to interstellar turbulence, which is constantly stirred by super-nova explosions. Multi-scale interactions are responsible for inevitably complex dynamics in these non-equilibrium systems, a proper understanding and description of which remains as a significant challenge in classical physics. As a remarkable consequence of multi-scale interactions, a quasi-equilibrium state can however be maintained by hovering around a *marginal* state by a continuous adjustment of perturbations to establish a new equilibrium [1]. While a small perturbation can be transported by the excitation of waves around a quiet equilibrium state, the relaxation of a large deviation can involve ballistic, avalanche-like events of large amplitude on a short dynamical time scale. This is an essential feature of the so-called self-organization, or self-organized criticality (SOC) in a more restricted sense [2]. In particular, it appears to be a powerful paradigm for understanding complexity in plasmas, with a growing body of supporting evidence for self organization from computer simulations, experiments, and observations in laboratory and astrophysical plasmas [3, 4, 5, 6, 7, 8, 9, 10].

The purpose of this paper is to provide a statistical theory of self organization, which can perhaps be utilized as an exploratory model in different contexts. As a concrete example, we consider a forced shear flow, whose gradient grows until it becomes unstable according to the stability criterion. For instance, in a strongly stably stratified medium, fluctuations on small scales (or internal gravity waves) will sharpen the structure of a shear flow u [11, 12], acting as a forcing, until its gradient $\partial_x u = u_x$ exceeds the critical value u_{xc} , set by Richardson criterion $R > R_c = (u_{xc}/\mathcal{N})^2 = 1/4$. Here \mathcal{N} is the buoyancy frequency due to the restoring force (buoyancy) in a stably stratified medium. Once it becomes unstable, the shear flow will relax its gradient rapidly and generate turbulence (fluctuations) until it starts building up again at the expense of fluctuations. In magnetically confined plasmas, poloidal shear flows (zonal flows) and/or parallel flows can be generated from drift waves while becoming subject to Kelvin-Helmholtz type instabilities [3, 13]. Although precise physical mechanisms for the generation and damping may differ, the repetition of growth and damping of shear flow is generic, occurring in many other systems, playing a crucial role in momentum transport, mixing, etc.

We model the essential physics involved in the self-organization alluded to above by the following one dimensional (1D) nonlinear diffusion equation for u_x [14],

$$\partial_t u_x = \partial_{xx}[D(u)u_x] + f, \quad (1)$$

where

$$D(u) = \nu + \beta u_x^2. \quad (2)$$

In Eqs. (1)-(2), f is an external forcing; $D(u)$ represents the effective diffusion coefficient including both the molecular diffusivity ν and nonlinear (eddy) diffusivity capturing relaxation process for unstable shear flow $|u_x| > u_{xc}$. A similar quadratic eddy diffusivity has widely been used in modelling chemical mixing and angular momentum transport (e.g. in stars and the Sun) although the precise value of parameter β has been controversial, often adjusted in an attempt to reproduce observational data [15].

Since the nonlinear diffusion in Eq. (2) becomes important for large gradient $|u_x| > \sqrt{\nu/\beta}$, inhibiting further increase in the gradient, the critical gradient is roughly $u_{xc} \sim \sqrt{\nu/\beta}$. Due to the relaxation of the gradient above this critical value, a *naive* expectation is that the value of gradient mostly remains subcritical. This would however be the case only when a relaxation time is sufficiently short compared with the characteristic time scale of the perturbation (forcing). In the realistic situation with continuous perturbation (a stochastic forcing), there will be a broad distribution of the gradient, some values of which may exceed far above its critical value. The key quantity to be determined is thus *the probability distribution function (PDF) of the gradient, rather than its average value*. In the following, we provide the first prediction of the PDF tails of the gradient by analytical and computational studies. Specifically, we show that PDFs tails for large $|u_x| > u_{xc}$ are strongly non-Gaussian (intermittent) with an exponential scaling $\exp(-cu_x^4)$ while near the center for small $|u_x| < u_{xc}$, PDFs are Gaussian $\exp(-cu_x^2)$ ($c = \text{constant}$). We then discuss a threshold model where $D(u)$ is given by discontinuous values to examine the validity of the nonlinear diffusion model, elucidating a crucial role of relative time scales of relaxation and disturbance in the PDFs. Note that there has been a growing interest in statistical analysis of SOC by using various statistical measures, including PDFs of avalanches [7, 8].

The remainder of the paper is organized as follows. We present analytical and numerical results of the PDFs of shear in a nonlinear diffusion model in §2. The predicted power

spectrum in this model is provided in §3. A threshold model is investigated in §4, with numerical results presented. Section 5 contains Conclusion.

II. PDFS OF SHEAR IN A NONLINEAR DIFFUSION MODEL

In this section, we provide analytical prediction and numerical simulation results of the PDFs of the shear u_x in a nonlinear diffusion model (1)-(2), in particular, showing the agreement on strongly intermittent exponential PDF tails of u_x .

A. Analytic result

Since for small $|u_x| \ll u_{xc}$, the forcing is balanced by linear diffusion, naturally leading to the Gaussian distribution of u_x , we focus on the PDF tails for large value of $|u_x|$ where the cubic nonlinearity becomes important. In order to incorporate this nonlinear interaction non-perturbatively, our key idea is to look for a nonlinear structure that is likely to be naturally sustained in a system. One candidate for such a nonlinear structure is an exact nonlinear solution $u_x \propto x$ to Eqs. (1)-(2) in the absence of the forcing. Due to a stochastic forcing, this structure is then likely to form in a random fashion with the temporal behaviour governed by $Q(t)$ as $u_x \sim iQ(t)x$. Note that similar coherent structures (ramps) have also been successfully used in the prediction of the intermittent PDF tails of (positive) velocity gradient in Burgers turbulence [16, 17] that agree with numerical results. The PDF of u_x then becomes equivalent to that of $Q(t)$, which satisfies:

$$\partial_t Q = -\beta Q^3 + g, \quad (3)$$

where g is the time dependent part of the forcing with the spatial profile $\propto x$. In the case of a temporally short-correlated forcing

$$\langle g(t_1)g(t_2) \rangle = \delta(t_1 - t_2)G, \quad (4)$$

the Fokker-Planck equation for the PDF of Q can be derived by using a standard technique [19]. To this end, we introduce the generating function $Z(\lambda, t) = e^{-i\lambda Q}$ to obtain

$$\partial_t \langle Z \rangle = \beta \lambda \partial_{\lambda \lambda \lambda} \langle Z \rangle - \lambda^2 G \langle Z \rangle, \quad (5)$$

where $\langle Z \rangle = \int dQ P(Q, t) e^{-i\lambda Q} = \tilde{P}(\lambda, t)$ is Z averaged over the forcing g , which is equal to Fourier transform of $P(Q, t)$. The Fourier transform of Eq. (5) then gives us the evolution equation for P as:

$$\partial_t P(Q, t) = \beta \partial_Q [Q^3 P] + G \partial_{QQ} P. \quad (6)$$

A stationary solution of Eq. (6) can easily be found to be $P(Q, t) \sim P_0 \exp[-\beta Q^4/(4G)]$, leading to

$$P(u_x; x, t) \sim P_0 \exp[-\beta u_x^4/4G]. \quad (7)$$

The PDFs tails in Eq. (7) are non-Gaussian, intermittent with the exponential scaling of $P \sim \exp(-\beta u_x^4/4G)$, and symmetric under the reflection $x \rightarrow -x$ (unlike Burgers turbulence [16, 17, 18] which is anti-symmetric). This exponential tail is one manifestation of intermittency caused by a coherent structure.

To complement the Fokker-Plank approach, it is instructive to consider an alternative non-perturbative method based on a path integral formulation [17, 20, 21, 22]. A key concept in this method is similar to what was alluded in our Fokker-Plank approach in that a temporally localized, nontrivial vacuum state with a coherent structure – the so-called instanton which maximizes the path integral – causes intermittency, contributing to the PDF tails. Main steps involved in the computation of the PDFs by the instanton method are as follows. First, we express the PDFs of the velocity gradient $u_x = v$ to take the value of A [$P(A)$] in terms of a path integral:

$$P(A) = \int d\lambda e^{i\lambda A - S_\lambda}, \quad (8)$$

where the effective action S_λ is given by

$$\begin{aligned} S_\lambda = & -i \int dx dt \bar{v} [\partial_t v - \partial_{xx}(\nu + \beta v^2)v] \\ & + \frac{1}{2} \int dx dy dt \bar{v}(x, t) \kappa(x - y) \bar{v}(y, t) \\ & + i\lambda \int dx dt v(x) \delta(x - x_0) \delta(t). \end{aligned} \quad (9)$$

Here, \bar{v} is the conjugate variable to $v = u_x$. By using the ansatz for temporally localized solutions $v = F(t)\phi$ and $\bar{v} = \mu(t)\bar{\phi}$ in Eq. (8) and then by maximizing the effective action S_λ with respect to F and μ , we obtain the equations for F and μ (with $\nu = 0$) as follows:

$$\partial_t F - \beta c_2 F^3 = -i c_3 \mu, \quad (10)$$

$$\partial_t \mu + 3\beta c_2 F^2 \mu = -\lambda c_4 \delta(t), \quad (11)$$

where

$$\begin{aligned}
c_1 &= \int dx \bar{\phi}(x) \phi(x), \\
c_1 c_2 &= \int dx \bar{\phi}(x) \partial_{xx} [\phi(x)^3], \\
c_1 c_3 &= \int dx dy \bar{\phi}(x) \kappa(x-y) \bar{\phi}(y), \\
c_1 c_4 &= \phi(x(t=0)) \equiv \phi(x_0).
\end{aligned} \tag{12}$$

Since instanton v propagates forward in time and its conjugate variable \bar{v} backward in time while the PDF is computed at $t = 0$, the boundary conditions on F and μ are:

$$F(-\infty) = 0, \quad \mu(t > 0) = 0. \tag{13}$$

For $t < 0$, Eqs. (10) and (11) give us the equation for $F(t)$ as

$$\partial_{tt} F = 3c_2 \beta^2 F^5, \tag{14}$$

which can be solved with the boundary conditions $F(t = 0) = F_0$ and $F(t \rightarrow -\infty) = 0$ [Eq. (13)];

$$F = \frac{F_0}{(1 + 2\beta c_2 F_0^2 t)^{1/2}}. \tag{15}$$

To find the value of F_0 , we integrate Eq. (11) for an infinitesimal time interval $t = [-\epsilon, \epsilon]$ by using Eq. (13) as:

$$\mu(-\epsilon) = \mu(0) = \lambda c_4, \tag{16}$$

and substitute Eq. (16) and $\partial_t F = -\beta c_2 F^3$ [from Eq. (15)] in Eq. (10) to obtain

$$F_0^3 = \frac{ic_3 c_4 \lambda}{2\beta c_2} \equiv q\lambda, \tag{17}$$

where $q = ic_3 c_4 / 2c_2 \beta$.

The determination of the PDFs of $P(A)$ now requires a few more steps. First, we evaluate S_λ in Eq. (8) by using Eqs. (15), (16) and (17):

$$S_\lambda = Q\lambda^{4/3}, \tag{18}$$

where $Q = 3i(c_1 c_4)q^{1/3}/4$. The next step is to find the PDF tails by computing the λ integral (8) in the limit of large λ . To this end, we substitute Eq. (18) into Eq. (8) and approximately evaluate λ integral as $\int d\lambda e^{i\lambda A - S_\lambda} \equiv \int d\lambda e^{-G(\lambda)} \sim e^{-G(\lambda_0)}$, where $G(\lambda) = -i\lambda A + S_\lambda$ and

$\lambda_0 = (3iA/4Q)^3$ is a saddle-point which minimizes $G(\lambda)$. Therefore, $P(A)$ in Eq. (8) becomes

$$P(A) \propto e^{-\xi \left(\frac{A}{\phi(x_0)}\right)^4}, \quad \xi = \frac{\beta}{2} \left| \frac{(c_2 c_1) c_1}{(c_3 c_1)} \right|. \quad (19)$$

Equation (19) is the exponential tail of PDF of u_x to take the value of A , with the same exponential scaling as in (7). Of importance to notice is that the result (19) follows from the order of the highest cubic nonlinearity in Eq. (1), being independent of the precise form of the spatial structure of ϕ and $\bar{\phi}$, which has not been specified yet. The latter however plays a crucial role in the determination of the overall amplitude of the PDFs through the coefficient ξ [see Eq. (19)]. Fortunately, the form of $\phi \propto x$ and $\bar{\phi} \propto x^3$ (i.e. the exact nonlinear solutions to v and \bar{v}) can be inferred from the instanton equations $\partial_t v - \partial_{xx}(\beta v^3) = -i \int dy \kappa(x-y) \bar{v}(y, t)$ and $\partial_t \bar{v} + \partial_{xx}(3\beta v^2 \bar{v}) = -\lambda v(x_0) \delta(t)$, obtained by minimizing S_λ with respect to v and \bar{v} , and by then using $\kappa(x-y) \sim \kappa_0[1 - (x-y)^2/2 + \dots] = \kappa_0[1 + xy + \dots]$. The use of $\phi \propto x$ and $\bar{\phi} \propto x^3$ in Eqs. (12) and (19) then gives $|c_2 c_1 / c_3| \sim 6/\kappa_0$, and thus $\xi \sim 3(\beta/\kappa_0)$.

To summarize, both Fokker-Planck and instanton methods, based on the key idea that the PDFs tails are caused by a coherent structure, give us the strongly intermittent PDFs tails of shear gradient u_x , with the same exponential scalings $\exp(-cu_x^4)$ ($c = \text{constant}$) [see Eqs. (7) and (19)]. It is interesting to compare these results with the right PDFs of the velocity gradient in Burgers turbulence, which was predicted to be exponential with a different exponent [i.e., $\exp(-cu_x^3)$] due to ramp-like coherent structures ($u \propto x$) [17] (followed by numerical verification). This scaling with the different exponent basically results from the quadratic highest nonlinear interaction in Burgers turbulence, different from the cubic highest interaction in our model (1)-(2) (see [21] for more details). In plasma turbulence, exponential PDFs tails of various fluxes have been theoretically predicted without numerical confirmation (e.g. see [20, 21, 22]). Nevertheless, it is very interesting that these exponential scalings have often been observed in the tails of fluxes in laboratory plasmas (e.g. see Refs. [23, 24]).

B. Numerical Results

To test our analytical prediction (7) and (19), we perform direct numerical simulations by numerically integrating Eqs. (1) and (2) using method outlined in [14]. To briefly recap, we use finite difference method to solve (1). The spatial discretization is second order accurate and the time integration uses Euler-Maruyama method. Adaptive time stepping is also used for numerical stability of the diffusion term. For each step of the simulations, the Gaussian noise is produced using the Box-Muller method [25], which gives homogeneous, and temporally short-correlated forcing f in Eq. (1) with the power spectrum $F(k)$:

$$\langle f(k_1, t_1)f(k_2, t_2) \rangle = \delta(t_1 - t_2)\delta(k_1 + k_2)F(k). \quad (20)$$

The results for the PDFs of u_x , $P(u_x)$, for a white-noise $F(k) = k^0$ are shown by the solid line in Fig. 1 for the values of parameters $\nu = 6 \times 10^{-3}$ and $\beta = 6.25 \times 10^{-3}$. It can clearly be seen that the PDF is Gaussian near the center but becomes exponential $\exp(-cu_x^4)$ in the tails ($c = \text{constant}$). These exponential tails agree perfectly with our theoretical prediction (7). To highlight this, the dotted and dashed lines in Fig. 1 are fits to a Gaussian and to $\exp(-cu_x^4)$, respectively. The cross-over between these two regimes occurs approximately at the expected critical gradient of $u_{xc} \simeq \sqrt{\nu/\beta} = 0.98$. The mean value of $|u_x|$ is found to be smaller than this, with the value about 0.59. However, there is yet a significant probability of 20% of super-critical gradient $|u_x| > |u_{xc}|$ from the PDF tails. The intermittent occurrence of super-critical gradients can be appreciated from the profile of u_x plotted in Fig. 2, which exhibits a bursty of large gradients. Reflectional symmetry of the PDF is also seen in Figs. 1 and 2.

While mathematically, the PDF tails $\exp(-cu_x^4)$ result from the highest cubic nonlinearity in the equation for u_x (1), physically, they are due to the feedback of shear on turbulence when it becomes unstable. That is, while shear is generated by turbulence [modelled by the forcing f in Eq. (1)], it feeds back on turbulence, limiting its own growth, thereby reducing the PDF tails below the Gaussian prediction (see Fig. 1). We have confirmed that these exponential PDFs tails are robust features by using different power spectra $F(k) \sim k^{-1}$ and k^{-2} .

III. POWER SPECTRUM IN A NONLINEAR DIFFUSION MODEL

One of the main interests in the previous studies of self-organization (or SOC) has been power spectrum. It is thus interesting to examine what prediction can be made on the power spectra in our model. To this end, we compute the PDFs of $u_x(k)$, i.e. $P(k, t)$ by observing that the evolution of k mode involves the cubic nonlinearity due to nonlinear diffusion in Eq. (2) of the form $\int dk_1 dk_2 u_x(k_1) u_x(k_2) u_x(k - k_1 - k_2)$. We approximate the latter as $|u_x(k)|^2 u_x(k)$ by keeping only the dominant coherent interaction (which can be justified for a narrow spectrum), and rewrite Eq. (1) as follows:

$$\partial_t u_x \simeq \beta k^2 u_x^3 - \nu k^2 u_x + f. \quad (21)$$

The Fokker-Planck equation for the $P(u_x; k, t)$ can be obtained as previously, from which a stationary PDF follows as:

$$P(u_x; k, t) = P_0(k) e^{-k^{2+r} u_x^2 (k^2 u_x^2 / 2 + \nu)}, \quad (22)$$

where $P_0(k) = 1 / \int du_x P(u_x; t)$ is the normalization constant, and the power spectrum $F(k) = k^{-r}$ is used. In the linear case, it is easy to see that the power spectrum $p(k) = \langle |u_x(k)|^2 \rangle = \int P(u_x; t) |u_x(k)|^2 \propto k^{-r-2}$. On the other hand, in a strongly nonlinear case, we find that

$$p(k) \propto k^{-(2+r/2)}. \quad (23)$$

Remarkably, the prediction (23) agrees very well with the numerical results shown in Liu [14]. In particular, in the case of the red noise with $r = 2$, Eq. (23) predicts k^{-3} spectrum, with a better agreement with numerical result than the prediction ($k^{-3.5}$) from the renormalization theory!

IV. THRESHOLD MODEL

Our results highlight the importance of the statistical description of self-organization. In particular, the population of super-critical gradients as well as the form of PDF tails can depend on the relative time scales between disturbance (i.e. forcing) and relaxation. To show this, we consider a threshold model where the nonlinear diffusion $D(u)$ in Eq. (1) is

given by the two discrete values as

$$D(u) = \begin{cases} \nu, & \text{for } |u_x| < u_{xc}; \\ V \ (\gg \nu), & \text{for } |u_x| > u_{xc}. \end{cases}$$

Here ν is molecular diffusivity while V represents a large diffusion due to avalanche-like events which efficiently relax super-critical gradients [14]. To investigate the extreme limit where the relaxation rapidly occurs on the shortest time scale, we numerically solve Eq. (1) by using this discrete $D(u)$ and by applying forcing when $|u_x|$ is less than u_{xc} everywhere in the domain in order to ensure that the relaxation occurs much faster than the disturbance. Note that a similar method was used, for example, in the SOC solar flare models [9, 10]. Numerical simulation results using $\nu = 6 \times 10^{-3}$, $V = 4.5 \times 10^{-2}$, and $u_{xc} = 2$ are plotted in Fig. 3, which shows that only 0.24% shear is super-critical. This is much less than 20% found in Fig. 1 in the nonlinear diffusion model, and is due to rapid relaxation by a large diffusion V for $|u_x|/u_{xc} > 1$. The resulting PDFs for this gradient $|u_x|/u_{xc} > 1$ are Gaussian as can be seen in Fig. 3 since the diffusion in Eq. (1) is essentially linear. In comparison, the Gaussian PDFs near the center for small $|u_x|/u_{xc} < 0.34$ results from small fluctuations which satisfy Gaussian statistics. What is very interesting is that there is a window of piece-wise exponentials $\exp(-cu_x^4)$ between these two Gaussian PDFs for the gradient $0.34 < |u_x|/u_{xc} < 1$, with a significant population 30%. This exponential PDFs are similar to those found in the nonlinear diffusion case for $|u_x|/u_{xc} > 1$ although the exact values of $|u_x|/u_{xc}$ for the exponential PDFs are not identical. Therefore, these results indicate that the nonlinear diffusion can be a reasonable approximation for a certain range of the shear values and relaxation time scales.

We have also performed the simulation by applying both the forcing and diffusive relaxation simultaneously to make disturbance time sufficiently short. The resulting PDFs are found to be Gaussian since the diffusion [Eq. (1)] in this case is essentially linear except at $|u_x| = u_{xc}$. The super-critical population is also higher (19%) due to the slower relaxation.

V. CONCLUSION

We have presented a statistical theory of self-organization by utilizing a simplified nonlinear diffusion model for a shear flow and a widely invoked quadratic eddy diffusivity [14, 15]. Both Fokker-Planck and instanton methods predict the PDF tails of the exponential form

$\exp(-cu_x^4)$, with a strong intermittency. Our numerical simulation using Gaussian forcing with three different power spectra not only confirm these predictions, but also reveal the significant contribution from the PDF tails with a large population of super-critical gradients, which could play a crucial role. These results highlight the importance of the statistical description of gradients in self-organization, rather than its average value as has conventionally been done. The validity of the nonlinear diffusion model was then examined using a threshold model, elucidating an important role of relative time scales of relaxation and disturbance, calling for a care in actual modelling of a particular system.

Our results can have significant implications for the dynamics and the role of shear flows (e.g. zonal flows) in laboratory, astrophysical and geophysical plasmas, which is vital not only in momentum transport, but also in transporting chemical species and controlling mixing of other quantities (e.g. air pollution, weather control) [26, 27]. Our theory can also provide a useful guide in understanding self-organization in other disciplines, such as population in environmental dynamics and biology, forest-fire, and reaction and diffusion in chemistry. Future work will include specific applications to those systems, the extension of our model to incorporate the finite correlation time of the forcing and a non-diffusive flux [28], and the investigation of the joint PDFs of fluctuations and mean gradients in a consistent way. Note that an initial attempt to the prediction of the joint PDFs has been made in the ion temperature gradient turbulence (for magnetically confined plasmas) by neglecting the feedback of shear flows on fluctuations [22, 29].

This research was supported by the EPSRC grant EP/D064317/1 and RAS Travel Grant. The National Center for Atmospheric Research is sponsored by the NSF.

-
- [1] K. Itoh, S.-I. Itoh, A. Fujiyama, and M. Yogi, *J. Plasma Fusion Res.* **79** 608 (2003).
 - [2] P. Bak, *Phys. Rev. Lett.* **59**, 381 (1987).
 - [3] C. Hildago, M. A. Pedrosa and B. Conclaves, *New J. Phys.* **4** 51 (2002).
 - [4] F. Sattin and M. Baiesi, *Phys. Rev. Lett.* **96** 105005 (2006).
 - [5] M. Paczuski, S. Botcher, and M. Baiesi, *Phys. Rev. Lett.*, **95**, 181102 (2005).
 - [6] X. Garbet, Y. Sarazin, F. Ibex, P. Gentry, C. Bordello, O. D. Garican, and P. H. Diamond,

- Phys. Plasmas, **14** 122305 (2007).
- [7] Y. H. Xu, S. Jachmich, R. R Weynants and the TEXTOR team, Plasma Phys. Control. Fusion, **47**, 1841 (2005).
- [8] P.A. Polizer, Phys. Rev. Lett., **84**, 1192 (2001); B.A. Carreras, B. van Milligen, C. Hidalgo, R. Bulbing, E. Sanchez, I. Garcia-Cortes, M. A. Pedrosa, J. Bluely and M. Endler, Phys. Rev. Lett., **83**, 3653 (1999).
- [9] H.-L. Liu, P. Charbonneau, A. Pouquet, T. J. Bogdan, and S. W. McIntosh, Phys. Rev. E., **66**, 056111 (2002).
- [10] P. Charbonneau, S. W. McIntosh, H.-L. Liu, and T. J. Bogdan, Solar Phys., **203**, 321 (2001).
- [11] E. Kim and K.B. MacGregor, Astrophys. J., **588**, 645 (2003).
- [12] E. Kim and N. Leprovost, Astron. & Astrophys., **468**, 1025 (2007).
- [13] B.N. Rogers, W. Dorland, and M. Goatskin, Phys. Rev. Lett., **81**, 5336 (2000).
- [14] H.-L. Liu, J. Atmospheric Sci., **64**, 579 (2007).
- [15] M.H. Pinsonnault, S. D. Kawaler, S. Sofia, and P. Demarque, Astrophys. J., **338**, 424 (1989).
- [16] A. Polyakov, Phys. Rev. E **52**, 6183 (1995).
- [17] V. Gurarie and A. Migdal, Phys. Rev. E **54**, 4908 (1996).
- [18] E. Balkovsky, G. Falkovich, I. Kolokolov, and V. Lebedev, Phys. Rev. Lett. **78**, 1452 (1997).
- [19] J. Zinn-Justin, *Quantum Field Theory and Critical Phenomena* (Clarendon Press, New York, 2002).
- [20] E. Kim and P.H. Diamond, Phys. Rev. Lett., **88**, 225002 (2002).
- [21] E. Kim and J. Anderson Phys. Plasmas, **15**, 114506 (2008).
- [22] J. Anderson and E. Kim, Phys. Plasmas, **15**, 082312 (2008).
- [23] J. R. Myra, D. A. Russell and D. A. D'Ippolito Phys. Plasmas, **15**, 032304 (2008).
- [24] S.J. Zweben, J. A. Boedo, O. Grille, C. Hidalgo, B. La Bombard, R. J. Magda, P. Scaring and J. L. Terry , Plasma Phys. Control. Fusion, **49**, S1 (2007).
- [25] W.H. Press, S.A. Teukolsky, W.T. Vetterling, and B.P. Flannery, *Numerical Recipes in Fortran Computing*, 2nd Ed. (Cambridge University Press, 1996), p919.
- [26] E. Kim, Phys. Rev. Lett., **96**, 084504 (2006).
- [27] N. Leprovost and E. Kim, Phys. Rev. Lett., **100**, 144502 (2008).
- [28] T.S. Hahm and P.H. Diamond, Phys. Plasmas, **2**, 580 (1995).
- [29] J. Anderson and E. Kim, Nucl. Fusion, "Non-perturbative statistical theory of intermittency

in ITG drift wave turbulence with zonal flows”, submitted (2009).

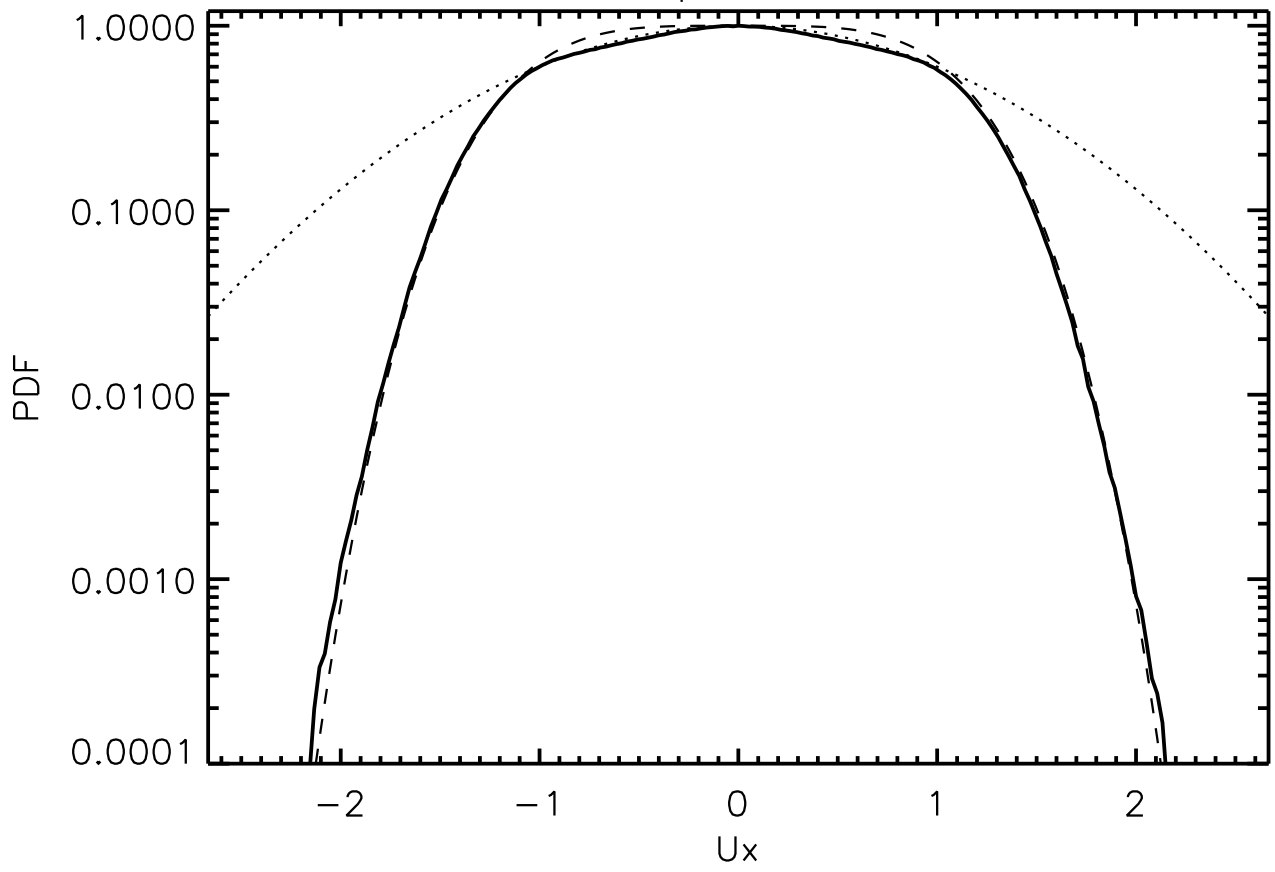
Figure Captions

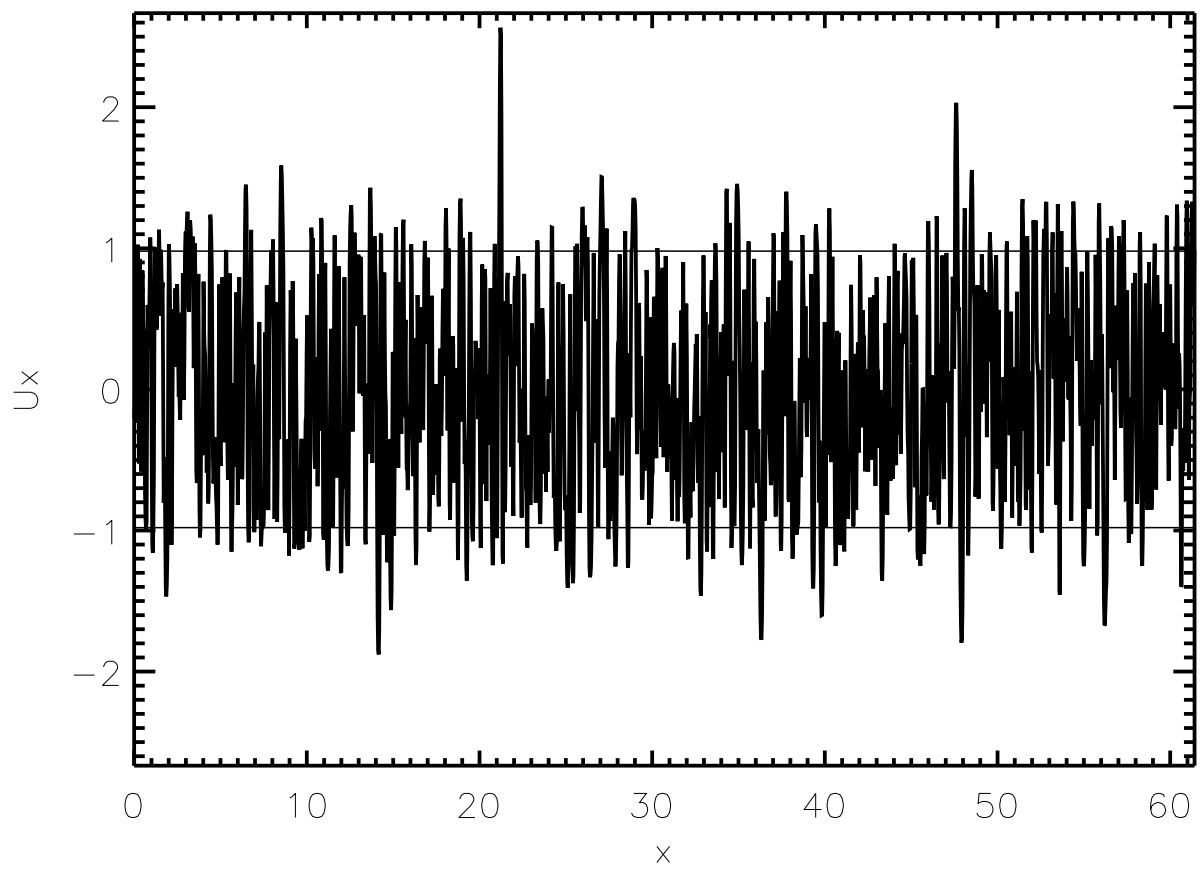
Fig. 1 The solid line is the PDFs from the numerical simulation of a nonlinear diffusion model (2) for a white noise. The dotted and dashed lines are the fits to Gaussian and $\exp(-cu_x^4)$ ($c = \text{const}$).

Fig2. The profile of u_x corresponding to Fig. 1.

Fig. 3 Solid line is the PDF from a threshold model. Dotted and dash-dotted-dotted-dotted lines are Gaussian fits; dashed and dashed-dotted lines are fits to $\exp(-cu_x^4)$ ($c = \text{const}$).

PDF of U_x , quadratic diffusion





PDF of U_x , threshold diffusion

